



© 2024 Geological Society of America. For permission to copy, contact editing@geosociety.org

Manuscript received 11 September 2023 Revised manuscript received 14 December 2023 Manuscript accepted 21 December 2023

Published online 16 January 2024

From dome to duplex: Convergent gravitational collapse explains coeval intracratonic doming and nappe tectonics, central Australia

Youseph Ibrahim^{1,*}, Patrice F. Rey¹, Donna L. Whitney², Christian Teyssier², Françoise Roger³, Valérie Bosse⁴, and Bénédicte Cenki³

¹School of Geosciences, University of Sydney, Sydney, NSW 2006, Australia

ABSTRACT

In central Australia, an apparently coeval gneiss dome (Entia Dome) developed adjacent to a thrust belt (Arltunga Nappe Complex) within an intracratonic setting. Here we employ a combination of fieldwork, geochronology, and numerical modeling to investigate the structure and tectonic evolution of these features. We present a structural model linking an extensional domain comprising the Entia Dome, across a transitional zone containing the Bruna décollement zone and the Illogwa shear zone, into a contractional zone comprising thrusts and duplexes of the Arltunga Nappe Complex. Supported by numerical modeling, we propose a tectonic model in which the dome and nappe complex formed synchronously because of the convergent gravitational collapse of the 30–40-km-deep Paleozoic Harts Range rift.

INTRODUCTION

Defying traditional plate tectonics, the Alice Springs orogeny developed between 450 and 300 Ma deep within the interior of the Australian continent (Fig. 1) at significant distances from any plate boundaries. It spans \sim 600 km, following a WNW-ESE-striking corridor amidst the weaker regions between the North, South, and West Australian cratons (Nixon et al., 2022). Before the Alice Springs orogeny, a large portion of the Australian Paleoproterozoic interior remained buried beneath the Neoproterozoic to Devonian Centralian Superbasin, remnants of which include the Amadeus Basin (Fig. 1). During much of the Paleozoic Era, Australia existed as a Gondwana promontory bordered by active margins on the NW (Metcalfe, 2021), N (Jost et al., 2018), and Pacific margins (Rosenbaum, 2018). Consequently, the intracratonic Alice Springs orogeny has been attributed to a combination of mantle dynamics (Houseman and Molnar, 2001; Roberts and Houseman, 2001) and far-field stresses (Klootwijk, 2013; Silva et al., 2018).

The region NE of the Amadeus Basin presents the intriguing geological association of the

Youseph Ibrahim **b** https://orcid.org/0000-0003-4803-5141

Entia gneiss dome, in which Paleoproterozoic upper amphibolite facies gneisses were exhumed alongside a series of nappes (Fig. 1). The nappe complex comprises the amphibolite to granulite facies rocks (10 kbar, 850 °C; Hand et al., 1999; Mawby et al., 1999) of the Harts Range Metamorphic Complex, the Paradise Nappes, and their lower-grade Neoproterozoic covers (Forman, 1971). These isoclinal fold nappes were thrust onto the greenschist facies Ruby Gap duplex and White Range duplex, which consist of Amadeus Basin sequences, overlapping the Amadeus Basin (Dunlap and Teyssier, 1995). Collectively, these nappes constitute the Arltunga Nappe Complex.

Understanding of the regional geology took a transformative turn when detrital zircon data revealed that the Harts Range Metamorphic Complex, into which the Entia Dome was emplaced, did not belong to the Paleoproterozoic basement. Instead, these gneisses are the metamorphic equivalent of Neoproterozoic to Paleozoic marine siliciclastic and limestone sediments of the Amadeus Basin with interlayered metavolcanics (Maidment et al., 2013; Tucker et al., 2015). Amphibolite to granulite facies metamorphism between 470 and 450 Ma is associated with bedding-parallel fabrics, suggesting syn-rift high-temperature (high-*T*) metamor-

phism within the Harts Range rift, a 30–40-km-deep sub-basin adjacent to the Amadeus Basin (Hand et al., 1999; Mawby et al., 1999; Maidment et al., 2005; Tucker et al., 2015). Granulite facies conditions seem to have been confined to deeper parts of the Harts Range rift, with little effect on the adjacent Paleoproterozoic basement (Mawby et al., 1999).

Episodic pegmatite emplacement between 450 and 300 Ma within the Entia Dome and the Harts Range Metamorphic Complex suggests the maintenance of high-*T* conditions in the deeper crust during most of the Paleozoic (Buick et al., 2008; Varga et al., 2022). Hence, the Entia Dome is a post–460 Ma structure that ascended through the Harts Range Metamorphic Complex during the Alice Springs orogeny. The driver for protracted partial melting following an episode of high-grade metamorphism in this intracontinental setting remains enigmatic (Buick et al., 2008; Asimus et al., 2023).

This paper focuses on the structure and tectonic history of the region between the Entia Dome and the Ruby Gap duplex across the intervening Illogwa shear zone (Fig. 1). We document a structural continuity from the Entia Dome to the Ruby Gap duplex and argue that the dome and duplex, active between 340 and 310 Ma, represent an extensional and contractional domain, respectively, linked by a translational domain that consists of the Bruna décollement zone and the Illogwa shear zone. We propose that the deep Harts Range rift basin led to a significant gravitational potential anomaly that relaxed via inward convergent gravitational collapse.

TRANSECT FROM DOME TO DUPLEX Entia Dome

The Entia Dome comprises migmatitic quartzofeldspathic gneisses and layered

CITATION: Ibrahim, Y., et al., 2024, From dome to duplex: Convergent gravitational collapse explains coeval intracratonic doming and nappe tectonics, central Australia: Geology, v. 52, p. 210–215, https://doi.org/10.1130/G51721.1

²Department of Earth and Environmental Sciences, University of Minnesota, Minneapolis, Minnesota 55455, USA

³Géosciences Montpellier, Université de Montpellier, CNRS, 34095 Montpellier cedex, France

⁴Laboratoire Magmas et Volcans, Campus Universitaire des Cézeaux, 63178 Aubière cedex, France

^{*}youseph.ibrahim@sydney.edu.au

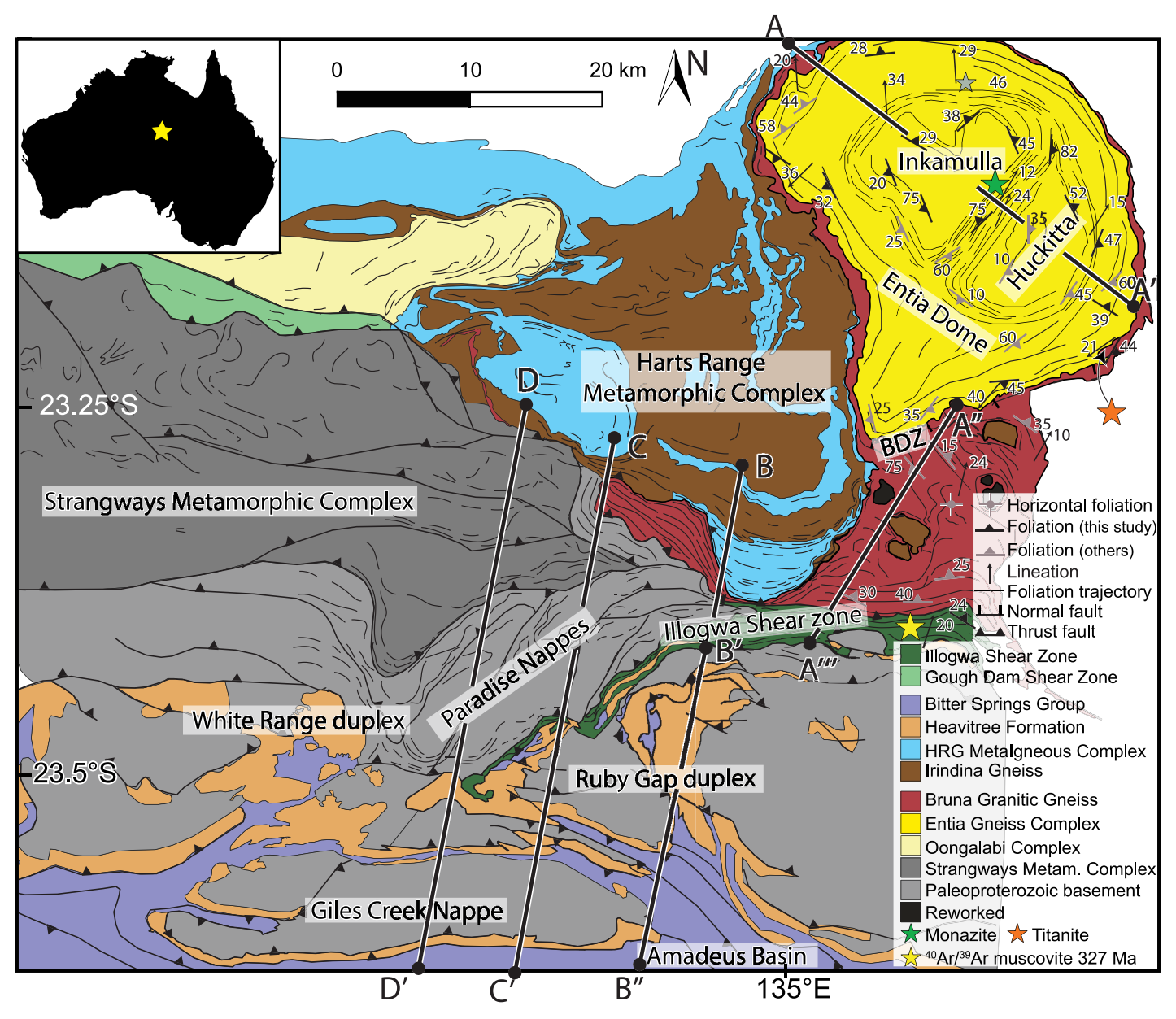


Figure 1. Geological map of the study area, central Australia, including location of geochronology data (40Ar/39Ar on muscovite from Reno and Fraser, 2021), using a combination of our own data and data from Forman (1971), Shaw et al. (1984), Shaw and Freeman (1990), and Dunlap (1992). HRG—Harts Range Group.

amphibolites and calc-silicates. A composite layer-parallel compositional banding fabric defines an internal architecture involving two subdomes separated by a planar high-strain zone (Figs. 1 and 2A). The subdome cores host the Huckitta and Inkamulla granodiorites dated (U-Pb zircon) at 1762 Ma and 1773 Ma. respectively (Maidment et al., 2005). Both granodiorites display a magmatic to solidstate fabric concordant with overlying migmatitic gneisses. On average, lineations within the dome trend to the NE (Fig. 1) and plunge 20°-30° to the NE. Polyphase structures in the migmatites show evidence of at least three fabric-forming events (Figs. 2D and 2E) with a clear regional partitioning. In the dome, the metatexite compositional layering and layerparallel foliation are folded into tight to isoclinal recumbent folds, ranging from centimeters to tens of meters in amplitude (Figs. S1A and S1B in the Supplemental Material¹). The subhorizontal migmatitic layering displays locally subhorizontal asymmetric boudinage and low-angle extensional shear bands with melt segregation that point to a strong extensional tectonic regime above the solidus (Fig. S1C). The magmatic fabric in the granodiorites preserves remnants of older structures (Fig. S2). At the margin of the dome, the recumbent folds are refolded by cascading recumbent folds (Fig. S3). Granite-bearing extensional fractures, some axial planar to these secondgeneration folds, show that these folds also developed at temperatures above the solidus (Figs. 2D and 2E). In between the subdomes, the high-strain zone records a strong horizontal NW-SE shortening, with tight to isoclinal upright folds (Fig. S4). The strain distribution is consistent with that expected during the exhumation of a migmatitic-cored dome, with

¹Supplemental Material. Additional field photographs, structural data, geochronology methodology and results, and additional information on the numerical modeling setup. Please visit https://doi.org/10.1130/GEOL.S.24891495 to access the supplemental material; contact editing@geosociety.org with any questions.

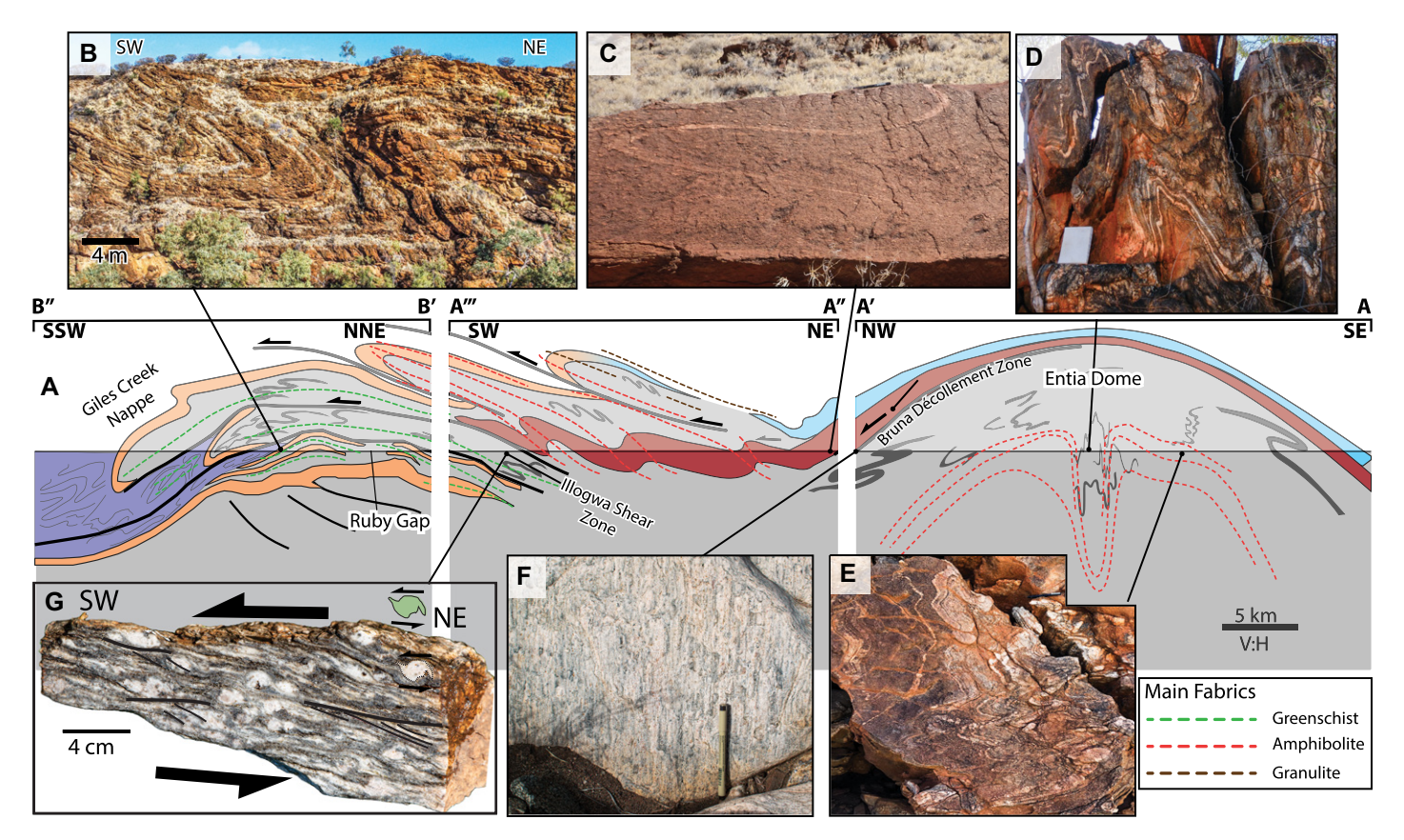


Figure 2. (A) Composite cross section from Ruby Gap Duplex to Entia Dome. Major thrust faults are shown as thick black lines. Lighter shading indicates interpretation above the current topography. The Harts Range Metamorphic Complex, including the Irindina Gneiss, is shown in light blue. Section lines and legend are shown in Figure 1. (B) Folds in the Bitter Springs Group. (C) Folded aplite vein with axial planar foliation in the Bruna décollement zone (pen for scale). (D, E) Upright folds (notebook for scale) (D) refolded into cascading folds (pen for scale) (E) in the high-strain dome envelope. (F) L-S tectonite within the Bruna décollement zone. (G) Kinematic indicators in the Illogwa shear zone.

vertical shortening and horizontal extension on top of the dome, gravity folding along its margin (Cruden, 1990), and horizontal shortening between the subdomes (Rey et al., 2017).

U-Pb ages of metamorphic monazite from Entia gneisses between 365 and 308 Ma (Wade et al., 2008, and references therein; Varga et al., 2021) as well as U-Pb ages of metamorphic zircon growth in the Huckitta Granodiorite at ca. 332 \pm 3 Ma (Maidment et al., 2005) and ca. 330 ± 6 Ma (Hand et al., 1999) point to a protracted metamorphism from 360 to 310 Ma, peaking at 7–9 kbar and 680-720 °C (Varga et al., 2021, and references therein) and melt-present conditions (Asimus et al., 2023). To better constrain the age of deformation, we conducted U-Th-Pb laser ablation-inductively coupled plasma-mass spectrometry (LA-ICP-MS) geochronology (Fig. S8) on monazite from a folded leucocratic vein within a metatexite between the subdomes (Figs. 1 and 2D; Fig. S4). Two distinct date populations identified at 339 ± 4 Ma and 314 ± 4 Ma as well as a concordant date at 365 ± 8 Ma are interpreted as representing two pulses of doming and melt extraction during a ca. 365 Ma to 310 Ma period of protracted metamorphism, melting, and deformation.

Southern Margin of the Entia Dome

The Bruna décollement zone deforms the contact between the Paleoproterozoic Entia gneisses and the Neoproterozoic to Paleozoic Irindina Gneiss at the base of the Harts Range Metamorphic Complex (Fig. 1) (James et al., 1989). Separating the basement and cover, the Bruna Granitic Gneiss (Fig. S5) has been interpreted as a ca. 1745 Ma (U-Pb zircon) laccolith (Ding and James, 1985; Mortimer et al., 1987; Cooper et al., 1988). The Bruna Granitic Gneiss records heterogeneous deformation (James et al., 1989). Along the S margin of the Entia Dome, the Bruna décollement zone corresponds to a prominent S-dipping normal shear zone. A strong L-S fabric carries a mineral and stretching lineation plunging to the SSW (Fig. 2F). Sm-Nd whole rock-garnet-hornblende isochron dating of Bruna Granitic Gneiss from the sheared NW margin of the Entia Dome yielded an age of 449 ± 10 Ma, interpreted to reflect a phase of Ordovician deformation (Mawby et al., 1999). Similar ages have been reported in the Harts Range (e.g., Buick et al., 2008). To constrain the age of shearing along the S margin of the dome, we have performed in situ LA-ICP-MS U-Pb dating of titanite from an isoclinally folded aplite vein (Fig. 2C) hosted in sheared Bruna

Granitic Gneiss (Fig. 1). We obtained a date of 315 ± 4 Ma (Fig. S8), interpreted as the minimum emplacement age for the vein and maximum age for shearing and folding, closely agreeing with the 314 ± 4 Ma age obtained in the high-strain zone between the subdomes.

South of the Entia Dome, the Bruna décollement zone flattens into a broad synform (Fig. 2A). The L-S fabric is flat lying, with the prominent stretching lineation gently plunging to the SSW or NNE. In some localities, strain shadows around K-feldspar and S-C fabrics in the Bruna Granitic Gneiss support a top-to-the-SW sense of shear (Figs. S6A and S6B). However, deformation was heterogeneous, varying in intensity and involving both simple and pure shear (Fig. S6C). The Bruna Granitic Gneiss thins out above the roof thrust of the Ruby Gap Duplex (Fig. 2).

Ruby Gap Duplex and the Illogwa Shear

South of the Bruna Granitic Gneiss, the Illogwa shear zone consists of quartzofeld-spathic gneisses and schists with mafic and calc-silicate interlayering, reminiscent of the rocks in the Entia Dome. The foliation dips 30°–50° to the N and carries a down-dip stretching and

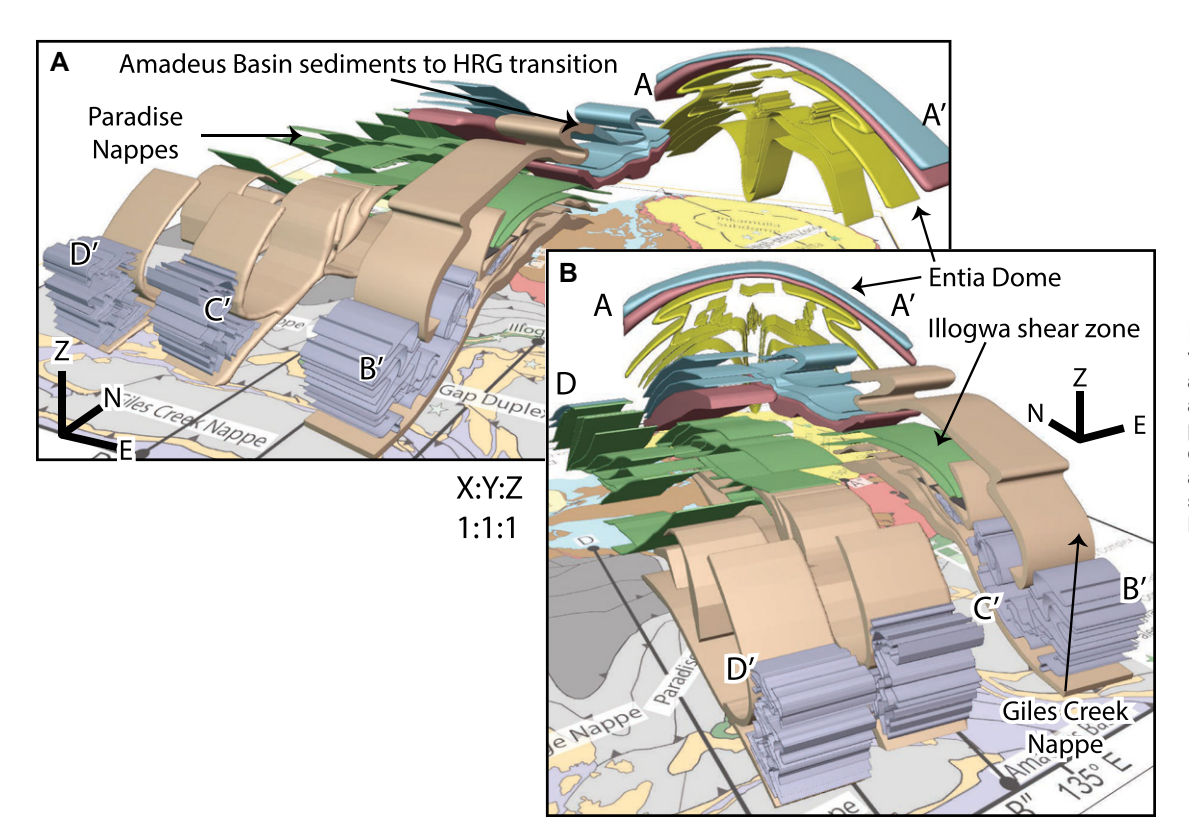


Figure 3. Two schematic views of the structural architecture of Entia Dome and Arltunga Nappe Complex. Paradise Nappes are colored green. Legend and section lines are shown in Figure 1. HRG—Harts Range Group.

muscovite lineation. We have observed S-C fabrics, δ -clasts, and σ -clasts recording clear top-to-the-SW kinematics (Fig. 2E; Fig. S7). This shear zone is in structural conformity with the overlying upper amphibolite facies Bruna décollement zone to the N and the underlying greenschist facies Ruby Gap duplex to the S. Although the Illogwa shear zone is commonly presented as a retrograde shear zone (Foden et al., 1995), it is part of an inverted metamorphic gradient linking the upper amphibolite facies fabric at the Entia Dome's S margin to the greenschist facies fabric of the Ruby Gap duplex (Collins and Teyssier, 1989; Dunlap and Teyssier, 1995). We speculate that the Illogwa shear zone fabric is the axial planar fabric of an anticlinal fold nappe made mainly of Paleoproterozoic gneisses, which may be structurally underneath the Paradise Nappes (Figs. 2 and 3). $^{207}\text{Pb}/^{206}\text{Pb}$ zircon ages of 1794 \pm 6 Ma and 1769 ± 3 Ma are interpreted as crystallization and later alteration ages, respectively. In contrast, the 327 \pm 2 Ma 40 Ar/ 39 Ar age obtained on muscovite (Reno and Fraser, 2021) defining the lineation (Fig. S7) can be interpreted as the age of the Alice Springs orogeny fabric.

Underneath and in structural conformity with the Illogwa shear zone, the Ruby Gap duplex is a S-directed duplex comprising Amadeus Basin sequences and the underlying Paleoproterozoic basement. To the W, it occupies the lowest structural level of the Arltunga Nappe Complex, underlying the Paradise and Harts Range Metamorphic Complex nappes and coeval with the structurally equivalent White Range duplex (Dunlap and Teyssier, 1995) (Fig. 1). To the first order, what is preserved is the duplicated limb of an anticlinal fold nappe (Fig. 2A). The basement and the competent Heavitree Formation are attached, and the overlying incompetent Bitter Springs Group (Fig. 2B) acts as a décollement. Thrusting occurred between 336 and 311 Ma (40 Ar/ 39 Ar on white mica) at temperatures straddling the ductile-brittle transition (250–300 °C; Dunlap, 1997). Under these conditions, thrust sheets internally deform by stretching in the transport direction.

Summary

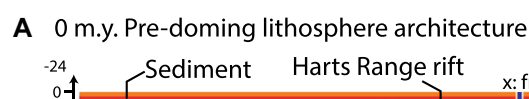
The structure across our transect consists of the Entia Dome, with a double-dome architecture, adjacent to the Arltunga Nappe Complex to the S comprising a stack of imbricated metamorphic fold nappes including the Illogwa shear zone (Figs. 2A and 3). The structural geology is conformal, with a progressive decrease in metamorphic conditions from upper amphibolite facies in the Entia Dome and the Bruna Granitic Gneiss to lower amphibolite facies across the Illogwa shear zone and greenschist facies in the Ruby Gap duplex (Figs. 2A and 3). Structures within the Entia Dome and the Bruna décollement zone developed under extension, while the Arltunga Nappe Complex developed under contraction. Exhumation of the Entia Dome, shearing along the Bruna décollement zone and Illogwa shear zone, and thrusting of the Arltunga Nappe Complex are age bracketed between ca.

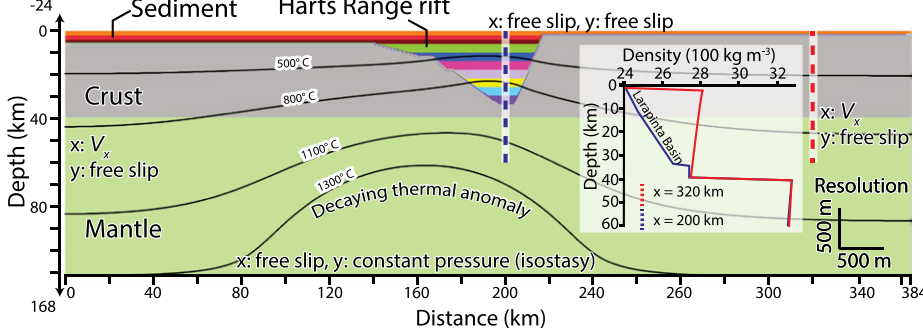
345 and ca. 310 Ma. The structural continuity and geochronology indicate that these features are synchronous and interrelated.

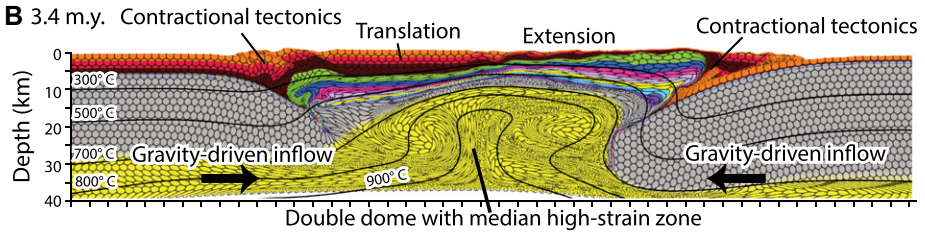
TECTONIC MODEL

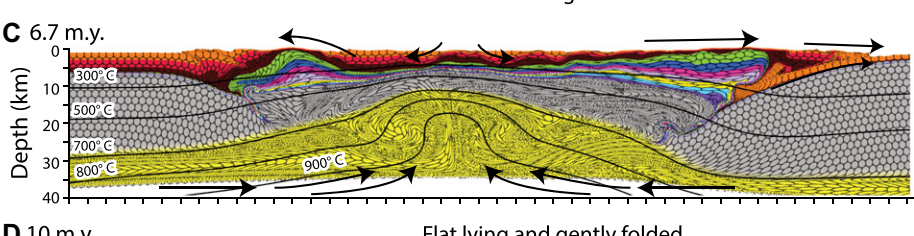
The Entia Dome was emplaced into the 30-40-km-deep Harts Range rift basin (i.e., Irindina province), the base of which reached granulite facies metamorphism and melting at ca. 470 Ma (Maidment et al., 2013; Tucker et al., 2015). The density contrast between the Neoproterozoic to Paleozoic sedimentary basin infill and the metamorphic Paleoproterozoic basement creates a strong horizontal pressure gradient, leading to significant gravitational stresses acting laterally toward the basin (Rey et al., 2001). As the geotherm in the basin reached melting conditions, these gravitational forces may have overcome viscous strength to drive centripetal flow, forcing the exhumation of the Entia Dome and the development of gravity nappes.

To test this hypothesis, we ran a set of thermo-mechanical numerical experiments using the Underworld framework (Moresi et al., 2007). The model setup comprises a 34-km-deep rift basin embedded into a metamorphic basement overlying a viscous mantle (Fig. 4A). The temperature field reflects conditions at ca. 470 Ma and delivers partial melting in the deeper level of the basin as well as the basement. Rheology is dependent on temperature, stress, strain, strain rate, and melt fraction. Detailed model information is provided in the Supplemental Material.









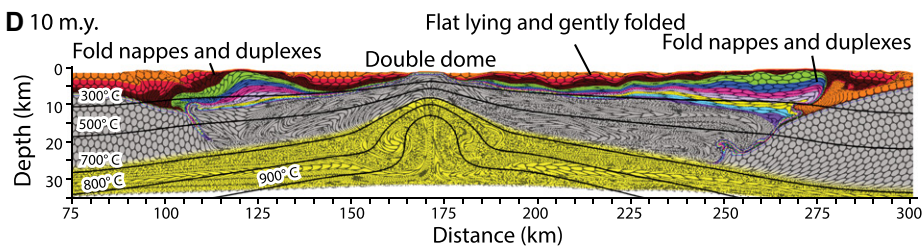


Figure 4. Numerical experiment showing contractional gravitational collapse of a deep and hot rift basin triggering exhumation of a gneiss dome and associated gravity nappes. (A) Initial model setup showing materials distribution, density profiles, boundary conditions, and isotherms. Velocity boundary condition V_x is applied to both vertical walls. V_x is compressional at 0.05 mm yr⁻¹ for 4 m.y. and extensional at 0.5 cm yr⁻¹ for the following 6 m.y. Decaying heat anomaly approximates temperature conditions associated with rifting. Blue and red dashed lines show locations of density profile. (B–D) Model evolution. Finite strain ellipses and isotherms are overlaid on the deforming material. Thin black arrows show flow direction.

We have tested static conditions and mild and faster convergent and divergent velocity conditions. All sets of experiments lead to the exhumation of a basement-cored double dome, pushing the basin infill upward and laterally into gravity nappes (Figs. 4B-4D). This experiment (Fig. 4) suggests that the contractional collapse of the Harts Range rift basin exhumed the Entia Dome and triggered S-SW gliding of gravitydriven fold nappes, accommodated by isoclinal folding and foliation-parallel slip. At cooler conditions, limbs of the isoclinal fold nappes were imbricated, forming the Ruby Gap duplex and White Range duplex. A transitional domain links the extensional exhumation of the dome to the contractional deformation at the front of the nappe complex (Fig. 4D). The delay between granulite facies conditions at 470-450 Ma and doming at ca. 340–310 Ma may be due to rifting's divergent velocity balancing the convergent gravitational velocity until ca. 355 Ma and slow conductive heating delaying basement weakening and convergent flow.

CONCLUSIONS

We propose a tectonic model linking the Entia Dome and the Ruby Gap duplex based on (1) the structural and metamorphic continuity between the dome and the duplex, (2) geochronological constraints showing synchronous dome exhumation and nappe emplacement from ca. 340 to ca. 310 Ma, and (3) coupled thermomechanical numerical experiments illustrating the geodynamics. Our model invokes the contractional gravitational collapse of the Neoproterozoic to Devonian Harts Range rift basin as

the driver for exhumation of the Entia dome, associated with gravitational spreading of the basin infill. This gravity-driven deformation was superimposed on far-field stresses driven by plate tectonics and may have contributed to deformation along the N margin of the Amadeus Basin. While the processes described here explain some Carboniferous features observed in the eastern Arunta region, it cannot explain the totality of the Alice Springs orogeny strain field.

ACKNOWLEDGMENTS

We acknowledge funding by Australian Research Council grants ARC-LP190100146 and ARC-DP220100709, and support by the Australian National Computational Infrastructure (NCI) National Computational Merit Allocation Scheme, Pawsey Supercomputing Centre, and Underworld provided by AuScope. Cenki received funding from European Horizon 2020 grant 793978. We thank our reviewers for their comments and insights.

REFERENCES CITED

Asimus, J.L., Daczko, N.R., and Ezad, I.S., 2023, Melt-present deformation at the Entia Dome, Central Australia: A metamorphic core complex formed during lower crustal tectonic extrusion: Lithos, v. 448–449, https://doi.org/10.1016/j.lithos.2023.107170.

Buick, I.S., Storkey, A., and Williams, I.S., 2008, Timing relationships between pegmatite emplacement, metamorphism and deformation during the intra-plate Alice Springs Orogeny, central Australia: Journal of Metamorphic Geology, v. 26, p. 915–936, https://doi.org/10.1111/j.1525-1314.2008.00794.x.

Collins, W.J., and Teyssier, C., 1989, Crustal scale ductile fault systems in the Arunta Inlier, central Australia: Tectonophysics, v. 158, p. 49–66, https://doi.org/10.1016/0040-1951(89)90314-4.

Cooper, J.A., Mortimer, G.E., and James, P.R., 1988, Rate of Arunta Inlier evolution at the eastern margin of the Entia Dome, central Australia: Precambrian Research, v. 40–41, p. 217–231, https://doi .org/10.1016/0301-9268(88)90069-1.

Cruden, A.R., 1990, Flow and fabric development during the diapiric rise of magma: The Journal of Geology, v. 98, p. 681–698, https://doi.org/10.1086/629433.

Ding, P., and James, P.R., 1985, Structural evolution of the Harts Range Area and its implication for the development of the Arunta Block, central Australia: Precambrian Research, v. 27, p. 251–276, https://doi.org/10.1016/0301-9268(85)90015-4.

Dunlap, W.J., 1992, Structure, kinematics, and cooling history of the Arltunga Nappe Complex, central Australia [Ph.D. thesis]: University of Minnesota, 276 p.

Dunlap, W.J., 1997, Neocrystallization or cooling?

⁴⁰Ar/³⁹Ar ages of white micas from low-grade mylonites: Chemical Geology, v. 143, p. 181–203, https://doi.org/10.1016/S0009-2541(97)00113-7.

Dunlap, W.J., and Teyssier, C., 1995, Thermal and structural evolution of the intracratonic Arltunga Nappe Complex, central Australia: Tectonics, v. 14, p. 1182–1204, https://doi.org/10.1029 /95TC00335.

Foden, J., Mawby, J., Kelley, S., Turner, S., and Bruce, D., 1995, Metamorphic events in the eastern Arunta Inlier, Part 2. Nd-Sr-Ar isotopic constraints: Precambrian Research, v. 71, p. 207–227, https://doi.org/10.1016/0301-9268(94)00062-V.

Forman, D.J., 1971, The Arltunga Nappe Complex, Macdonnell Ranges, Northern Territory, Austra-

- lia: Journal of the Geological Society of Australia, v. 18, p. 173–182, https://doi.org/10.1080/00167617108728756.
- Hand, M., Mawby, J.O., Kinny, P., and Foden, J., 1999, U-Pb ages from the Harts Range, central Australia: Evidence for early Ordovician extension and constraints on Carboniferous metamorphism: Journal of the Geological Society, v. 156, p. 715-730, https://doi.org/10.1144/gsjgs.156 .4.0715.
- Houseman, G., and Molnar, P., 2001, Mechanisms of lithospheric rejuvenation associated with continental orogeny, in Miller, J.A., et al., eds., Continental Reactivation and Reworking: Geological Society, London, Special Publication 184, p. 13–38, https://doi.org/10.1144/GSL.SP.2001 .184.01.02.
- James, P.R., Macdonald, P., and Parker, M., 1989, Strain and displacement in the Harts Range detachment zone: A structural study of the Bruna Gneiss from the western margin of the Entia Dome, central Australia: Tectonophysics, v. 158, p. 23–48, https://doi.org/10.1016 /0040-1951(89)90313-2.
- Jost, B.M., Webb, M., and White, L.T., 2018, The Mesozoic and Palaeozoic granitoids of north-western New Guinea: Lithos, v. 312–313, p. 223–243, https://doi.org/10.1016/j.lithos.2018.04.027.
- Klootwijk, C., 2013, Middle–Late Paleozoic Australia-Asia convergence and tectonic extrusion of Australia: Gondwana Research, v. 24, p. 5–54, https://doi.org/10.1016/j.gr.2012.10.007.
- Maidment, D.W., Hand, M., and Williams, I.S., 2005, Tectonic cycles in the Strangways Metamorphic Complex, Arunta Inlier, central Australia: Geochronological evidence for exhumation and basin formation between two high-grade metamorphic events: Australian Journal of Earth Sciences, v. 52, p. 205–215, https://doi.org/10.1080/08120090500139414.
- Maidment, D.W., Hand, M., and Williams, I.S., 2013, High grade metamorphism of sedimentary rocks during Palaeozoic rift basin formation in central Australia: Gondwana Research, v. 24, p. 865– 885, https://doi.org/10.1016/j.gr.2012.12.020.
- Mawby, J., Hand, M., and Foden, J., 1999, Sm-Nd evidence for high-grade Ordovician metamorphism in the Arunta Block, central Australia: Journal of

- Metamorphic Geology, v. 17, p. 653–668, https://doi.org/10.1046/j.1525-1314.1999.00224.x.
- Metcalfe, I., 2021, Multiple Tethyan ocean basins and orogenic belts in Asia: Gondwana Research, v. 100, p. 87–130, https://doi.org/10.1016/j.gr.2021.01.012.
- Moresi, L., Quenette, S., Lemiale, V., Mériaux, C., Appelbe, B., and Mühlhaus, H.-B., 2007, Computational approaches to studying non-linear dynamics of the crust and mantle: Physics of the Earth and Planetary Interiors, v. 163, p. 69–82, https://doi.org/10.1016/j.pepi.2007.06.009.
- Mortimer, G.E., Cooper, J.A., and James, P.R., 1987, U-Pb and Rb-Sr geochronology and geological evolution of the Harts Range ruby mine area of the Arunta Inlier, central Australia: Lithos, v. 20, p. 445–467, https://doi.org/10.1016/0024-4937(87)90029-6.
- Nixon, A.L., Glorie, S., Fernie, N., Hand, M., De Vries Van Leeuwen, A.T., Collins, A.S., Hasterok, D., and Fraser, G., 2022, Intracontinental fault reactivation in high heat production areas of central Australia: Insights from apatite fission track thermochronology: Geochemistry, Geophysics, Geosystems, v. 23, https://doi.org/10.1029/2022GC010559.
- Reno, B.L., and Fraser, G.L., 2021, Summary of results—Joint NTGS-GA geochronology project: Constraining cooling and deformation in the eastern Aileron Province through 40 Ar/39 Ar stepheating of hornblende, muscovite, and biotite: Northern Territory Geological Survey Record 2021-001, https://geoscience.nt.gov.au/gemis/ntgsjspui/handle/1/91246.
- Rey, P., Vanderhaeghe, O., and Teyssier, C., 2001, Gravitational collapse of the continental crust: Definition, regimes and modes: Tectonophysics, v. 342, p. 435–449, https://doi.org/10.1016/S0040-1951(01)00174-3.
- Rey, P.F., Mondy, L., Duclaux, G., Teyssier, C., Whitney, D.L., Bocher, M., and Prigent, C., 2017, The origin of contractional structures in extensional gneiss domes: Geology, v. 45, p. 263–266, https://doi.org/10.1130/G38595.1.
- Roberts, E.A., and Houseman, G.A., 2001, Geodynamics of central Australia during the intraplate Alice Springs Orogeny: Thin viscous sheet models, *in* Miller, J.A., et al., eds., Continental Reactivation and Reworking: Geological Society,

- London, Special Publication 184, p. 139–164, https://doi.org/10.1144/GSL.SP.2001.184.01.08.
- Rosenbaum, G., 2018, The Tasmanides: Phanerozoic tectonic evolution of eastern Australia: Annual Review of Earth and Planetary Sciences, v. 46, p. 291–325, https://doi.org/10.1146/annurev-earth -082517-010146.
- Shaw, R.D., and Freeman, M.J., 1990, Quartz, Northern Territory, sheet 5951: Australia Bureau of Mineral Resources, Geology and Geophysics, scale 1:100,000, https://geoscience.nt.gov.au/gemis/ntgsjspui/handle/1/81611.
- Shaw, R.D., Stewart, A.J., and Rickard, M.J., 1984, Arltunga–Harts Range region, Northern Territory: Australia Bureau of Mineral Resources, Geology and Geophysics, scale 1:100,000, https://geoscience.nt.gov.au/gemis/ntgsjspui/handle/1/81909.
- Silva, D., Piazolo, S., Daczko, N.R., Houseman, G., Raimondo, T., and Evans, L., 2018, Intracontinental orogeny enhanced by far-field extension and local weak crust: Tectonics, v. 37, p. 4421– 4443, https://doi.org/10.1029/2018TC005106.
- Tucker, N.M., Hand, M., and Payne, J.L., 2015, A rift-related origin for regional medium-pressure, high-temperature metamorphism: Earth and Planetary Science Letters, v. 421, p. 75–88, https:// doi.org/10.1016/j.epsl.2015.04.003.
- Varga, J., Raimondo, T., Morrissey, L., Kelsey, D.E., and Hand, M., 2021, Pressure–temperature–time constraints on gneiss dome formation in an intracontinental orogen: Journal of Metamorphic Geology, v. 40, p. 457–488, https://doi.org/10 .1111/jmg.12635.
- Varga, J., Raimondo, T., Hand, M., Curtis, S., and Daczko, N., 2022, Hydration, melt production and rheological weakening within an intracontinental gneiss dome: Lithos, v. 432–433, https:// doi.org/10.1016/j.lithos.2022.106872.
- Wade, B.P., Hand, M., Maidment, D.W., Close, D.F., and Scrimgeour, I.R., 2008, Origin of metasedimentary and igneous rocks from the Entia Dome, eastern Arunta region, central Australia: A U-Pb LA-ICPMS, SHRIMP and Sm-Nd isotope study: Australian Journal of Earth Sciences, v. 55, p. 703–719, https://doi.org/10.1080 //08120090801982868.

Printed in the USA